Measurement of Pion Transparency in Nuclei

Submitted by

K.R. Garrow (Spokesperson)
TRIUMF, Vancouver, CA

R. Carlini, D. Gaskell, D.G. Meekins, R. Ent (Co-spokesperson),H. C. Fenker,
M.K. Jones, A. Lung, D. Mack, G. Smith, S.A. Wood, and W.F. Vulcan
TJNAF, Newport News, VA

J. Arrington
Argonne National Laboratory, Argonne, IL

D. Dutta (Co-spokesperson) H. Gao, K. Kramer, X. Qian, W. Xu, Q. Ye, X. Zong
Duke University, Durham, NC

P. Markowitz
Florida International University, University Park, FL

O.K. Baker, M.E. Christy, L. Cole, A. Gasparian, P. Gueye,
B. Hu, C. Jackson, C.E. Keppel, V. Nazaryan, and L. Tang
Hampton University, Hampton, VA

K.G. Fissum
Lund University, Lund, Sweden

B. Clasie, H. Gao, J. Seely
Massachusetts Institute of Technology, Cambridge, MA

P. Bosted
University of Massachusetts, Amherst, MA

A. Borissov, W. Lorenzon
University of Michigan, Ann Arbor, MI

G.M. Huber

University of Regina, Regina, Saskatchewan, Canada

D. Day, N. Fomin
University of Virginia, Charlottesville, VA

R. Asaturyan, H. Mkrtchyan, S. Stepanyan, V. Tadevosyan
Yerevan Physics Institute, Yerevan, Armenia

Abstract

We propose to measure pion electroproduction off ^{1}H, ^{2}H, ^{12}C, ^{64}Cu, and ^{197}Au, and extract the pion transparency through the nuclear medium between $Q^2 = 1$ and 5 (GeV/c)^2. The pion transparency is predicted to be a signature of the onset of nuclear filtering and/or Color Transparency. Recent experiments have reported evidence for Color Transparency effects at $Q^2 \simeq 10$ (GeV/c)^2. The occurrence of nuclear filtering could potentially explain the apparent discrepancy between (proton) nuclear transparencies found in quasielastic A(e,e′p) and A(p,2p) experiments. The occurrence of these effects is an effective signature of the approach to the factorization regime in meson electroproduction experiments, necessary for the access to Generalized Parton Distributions. Measurable effects of ≈40% are predicted for this region of Q^2. The proposed experiment seeks to measure the pion transparency with 5-10% uncertainties, dominated by systematics, up to $Q^2 = 5$ (GeV/c)^2.

1 Introduction

Recently, QCD factorization theorems were derived for various deep inelastic exclusive processes [1, 2, 3, 4]. These factorization theorems are intrinsically related to the access to Generalized Parton Distributions (GPD's), introduced by Ji and Radyushkin [5, 6]. The discovery of these GPD's and their connection to certain totally exclusive cross sections has made it possible in principle to rigorously map out the complete nucleon wave functions themselves. The GPD's contain a wealth of information about the transverse momentum and angular momentum carried by the quarks in the proton. Presently, experimental access to such GPD's is amongst the highest priorities in intermediate energy nuclear/particle physics.

It is still uncertain at which Q^2 value one will reach the factorization regime, where the leading-order perturbative QCD domain fully applies for meson electroproduction. However, it is expected to be between $Q^2 = 5$ and 10 (GeV/c)^2. For example, it is generally believed that the pion elastic form factor is dominated by long-distance confinement-based physics for $Q^2 < 10$ (GeV/c)^2. Nonetheless, Eides, Frankfurt, and Strikman [7] point out that

"It seems likely that a *precocious factorization* ... could be valid already at moderately high Q^2 [≥ 5 (GeV/c)^2], leading to precocious scaling of the spin asymmetries and of the ratios of cross sections as function of Q^2 and x".

It is a little realized fact [8] that factorization is rigorously not possible without the onset of the Color Transparency (CT) phenomenon [9] (although, as mentioned, one can have precocious factorization). In addition to factorization, strict determination of GPD's will require that the wave functions being probed have evolved to their asymptotic form, or, alternatively, that one knows the exact (non-asymptotic) meson wave function. Note that the underlying assumption here is that in exclusive "quasielastic" meson production the meson is produced at small interquark distances.

CT was first discussed in terms of perturbative QCD considerations. However, later work [10] indicates that this phenomenon occurs in a wide variety of model calculations with nonperturbative reaction mechanisms. The existence of CT requires that high momentum transfer scattering should take place via selection of amplitudes in the initial and final state hadrons characterized by a small transverse size. Secondly, this small object should be 'color neutral' outside of this small radius in order not to radiate gluons. Finally, this compact size must be maintained for some distance in traversing the nuclear medium. Unambiguous observation of CT would provide a new means to study the strong interaction in nuclei.

Intuitively, one expects an earlier onset of CT for meson production than for hard proton scattering, as it is much more probable to produce a small transverse size in a $q\bar{q}$ system than in a three quark system (Evolution distances are presumed to be $2p_\pi/\Delta M^2$, with ΔM the mass difference between the pion and its lowest-lying a_2 Regge partner, and are easily larger than the nuclear radius). Recent support for CT comes from the coherent diffractive dissociation of 500 GeV/c negative pions into di-jets [11]. The inferred Q^2 for this reaction was ≥ 7 (GeV/c)^2. The A-dependence of the data was fit assuming $\sigma \propto A^\alpha$ for two k_t bins, with k_t the jet transverse momentum. For $1.25 < k_t < 1.5$, $1.5 < k_t < 2.0$ and $2.0 < k_t < 2.5$ ($Q^2 \geq 4k_t^2$) the alpha values were determined to be α=$1.64^{+0.06}_{-0.12}$, α=1.52$\pm$0.12, and α=1.55$\pm$0.16, respectively, far larger than the $\sigma \propto A^{0.7}$ dependence typically observed in inclusive π-nucleus scattering, whereas the theoretical [12] CT values were predicted to be α = 1.25, 1.45 and 1.60, respectively. However, this data does not inform about the kinematic onset of CT. Furthermore, all measurements to date yet have to answer whether CT is also a characteristic of nonperturbative QCD.

Thus, assuming that we take the conclusion from these di-jet data for granted, the CT phenomenon, and thus the onset of factorization, has to happen before $Q^2 = 10$ (GeV/c)^2. Therefore, one would anticipate the region between $Q^2 = 1$ (GeV/c)^2 and 10 (GeV/c)^2 to be the region of interest to look for such onset. [Note that if, on the other hand, one would take the approach that higher-twist contributions through, e.g., the quark transverse momentum $k_\perp$, should be small, factorization in meson electroproduction may still be questionable at such Q^2. These contributions are still predicted to be appreciable, a factor of $\approx$ 2-3, for $Q^2 \approx$ 3-10 (GeV/c)^2 [13, 14]].

It has been predicted [15] that exclusive processes in a nuclear medium are cleaner than the corresponding processes in free space. Large quark separations may tend not to propagate significantly in the strongly interacting medium. Configurations of small quark separations, on the other hand, will propagate with small attenuation. This phenomenon is termed nuclear filtering, and is the complement of CT. If such nuclear filtering occurs, the nuclear medium A should eliminate the long distance amplitudes. Thus, in the large A limit, one is left with a perturbatively calculable limit.

Such nuclear filtering could, e.g., explain the apparent contradiction between the proton transparency results from A(p,2p) and A(e,e$'$p) experiments: The nuclear transparency measured in A(p,2p) at Brookhaven [16, 17] has shown a rise consistent with CT for Q$^2 \simeq$ 3 - 8 (GeV/c)^2, but decreases at higher momentum transfer. The A(e,e$'$p) measurements at SLAC [18] and JLab [19, 20] yielded distributions in missing energy and momentum completely consistent with conventional nuclear physics predictions and the extracted transparencies exclude sizable CT effects up to $Q^2 = 8$ (GeV/c)^2. The resolution [15] may be that the interference between short and long distance amplitudes in the free p-p cross section are responsible for these energy oscillations, where the nuclear medium acts as a filter for the long distance amplitudes. [Still, questions remain with the recent claim that the nuclear transparencies at $Q^2 \simeq 8$ (GeV/c)^2 in A(p,2p) experiments deviate from Glauber predictions [17]].

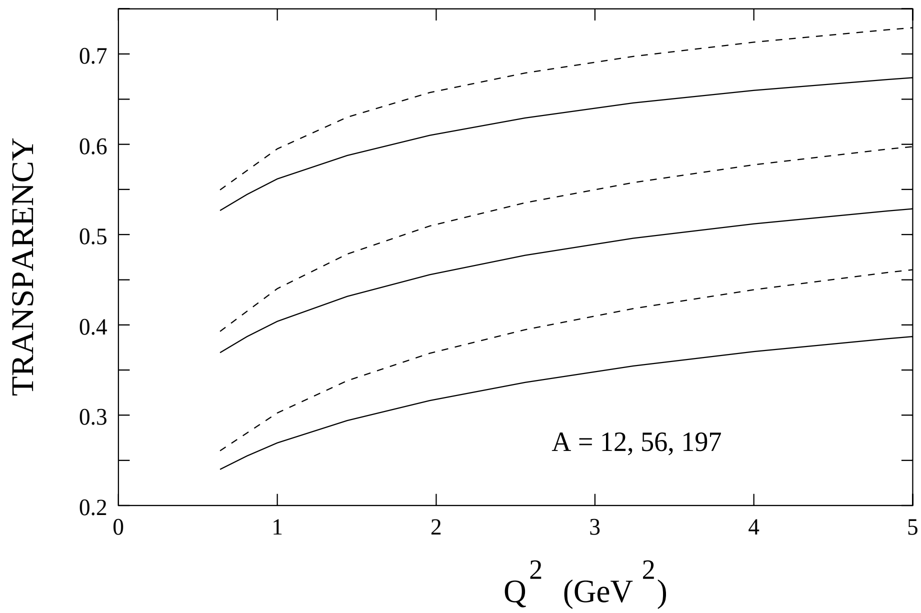

Figure 1: The calculated pion transparency ratio for different nuclei as a function of Q^2 [21]. The solid and dashed curves use the CZ and asymptotic distribution amplitudes, respectively, and correspond to $A = 12$, 56, and 197 from top to bottom.

Kundu *et al.* uses this idea to calculate pion transparency in electroproduction experiments [21]. Their calculation follows a perturbative QCD approach in the Impulse Approximation. Due to the hard scattering, only the short distance distribution amplitudes dominate. Size fluctuations or diffusion in the quantum mechanical propagation of quarks sideways and longitudinally is included in the perturbative treatment. The effects of interaction with the nuclear medium is included through an eikonal form. The calculation has to make an assumption on the distribution amplitudes. It appears [21] perturbative QCD effects are better applied to the nuclear medium, due to suppression of long distance components, and that CT effects are slower for end point-dominated distributions, of e.g. [22, 23]. Thus, we will use the latter calculations as a guideline to our choice of Q^2. Note that this approach is consistent with the assumption of CT at $Q^2 = 10$ (GeV/c)^2, as claimed by the di-jet experiment [11], and with the recent nuclear transparency results from the A(e,e$'$p) experiments [20]. For the latter case, the calculation would predict only of order 10% effects at $Q^2 \approx 30$ (GeV/c)^2.

We show, in Fig. 1, the calculated pion transparency ratio for the ^{12}C, ^{56}Fe, and ^{197}Au nuclei, as a function of Q^2, from [21]. As one can see, we would obtain a measurable effect, of $\approx 40\%$, for the Q^2 range between 1 and 5 (GeV/c)^2.

Please note that, as the elementary pion electroproduction process is not known in detail, a reliable "baseline" calculation without CT effects is an issue. CT effects can only unambiguously be verified as a deviation from a baseline nuclear physics calculation. Thus, a Q^2 dependence of the pion transparency in nuclei may also be introduced by conventional nuclear physics effects. However, the absolute value of the effects we are after also seems verified by an independent calculation by Miller [24]. In Fig. 2 we show the results of this pion transparency calculation for ^{12}C(e,e$'\pi^+$), at $Q^2 = 2$ (GeV/c)^2, as a function of the pion momentum p_π. One can see of order 10% effects in the absolute value of the pion transparency, due to the CT effect, at this Q^2. In the experiment proposed here we would probe the transparency at varying (Q^2,p_π) values.

2 The Experiment

The proposed experiment will measure the (e,e$'\pi^+$) cross section as a function of A and Q^2, up to Q^2 = 5 (GeV/c)^2. In general, the experiment will compare the ^{1}H(e,e$'\pi^+$) and ^{2}H(e,e$'\pi^+$) yields with the electroproduction yields of ^{12}C(e,e$'\pi^+$), ^{64}Cu(e,e$'\pi^+$), and ^{197}Au(e,e$'$p) at identical kinematics.

We intend to use 4 cm long cryogenic hydrogen and deuterium targets, Al dummy targets for window subtraction, a solid ^{12}C foil of 2% radiation length, a solid ^{64}Cu foil of 6% radiation length, and a solid ^{197}Au foil of 12% radiation length. These targets have been standard available for Hall C experiments.

The SOS and HMS spectrometers in Hall C will be used to detect the scattered electron and the electroproduced charged pion, respectively.

In the remainder of this Section we will describe how we intend to determine the pion transparencies. For this, we greatly benefit from expertise

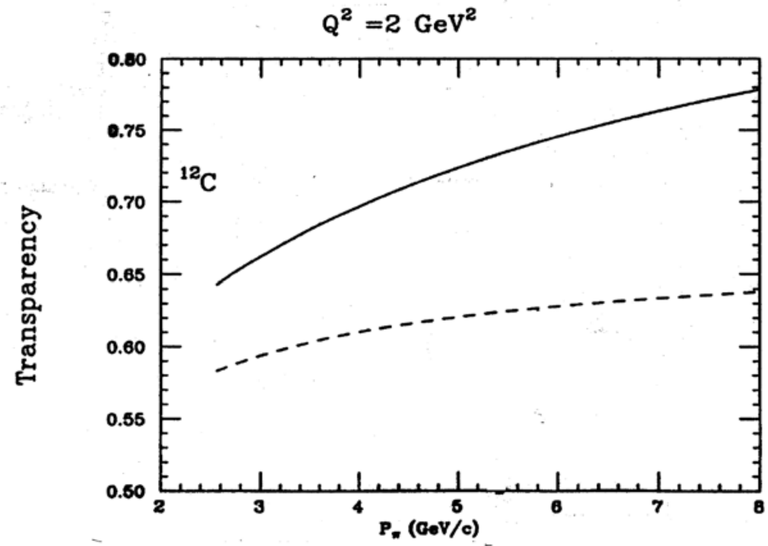

Figure 2: The calculated pion transparency ratio for ^{12}C(e,e$'\pi^+$) at $Q^2 = 2$ (GeV/c)^2 by Miller [24]. The dashed line indicates the Glauber-type DWIA calculation, the solid line indicates the calculation with CT effect. The pion momentum p_π varies the expansion length, for fixed Q^2 and virtual pion momentum k (= 0.4 GeV/c).

obtained in the E91-003 ("A Study of Longitudinal Charged Pion Electroproduction in ^{2}D, ^{3}He, and ^{4}He", spokesperson H.E. Jackson) and E91-016 ("Electroproduction of Kaons and Light Hypernuclei", spokespersons B. Zeidman and J. Reinhold) experiments.

The pion electroproduction cross section can be written as the product of a virtual photon flux (Γ) and a virtual photon cross section (evaluated in the laboratory frame),

$$\frac{d\sigma}{d\Omega_e dE_e d\Omega_\pi dM_x} = \Gamma \frac{d\sigma}{d\Omega_\pi dM_x} \,, \qquad (1)$$

where M_x is the missing mass of the recoiling system, $M_x^2 = (q + P_A - p_\pi)^2$. The virtual photon flux is given by

$$\Gamma = \frac{\alpha}{2\pi^2} \frac{E_e'}{E_e} \frac{1}{Q^2} \frac{1}{1-\epsilon} \frac{W^2 - M^2}{2M} \,. \qquad (2)$$

We take M to be the proton mass so that equal laboratory cross sections result in equal virtual photon cross sections regardless of target mass. The virtual photon cross section can be written as

$$\begin{aligned}\frac{d\sigma}{d\Omega_\pi dM_x} &= \frac{d\sigma_T}{d\Omega_\pi dM_x} + \epsilon\frac{d\sigma_L}{d\Omega_\pi dM_x} + \epsilon\frac{d\sigma_{TT}}{d\Omega_\pi dM_x}\cos 2\phi_{pq} \\ &+ \sqrt{2\epsilon(1+\epsilon)}\frac{d\sigma_{LT}}{d\Omega_\pi dM_x}\cos\phi_{pq}\ , \end{aligned} \tag{3}$$

where ϵ describes the longitudinal polarization of the virtual photon. In the parallel kinematics we will choose, the interference terms (σ_{LT} and σ_{TT}) are small, and for complete ϕ_{pq} coverage integrate to zero.

To compare the cross sections from H, ^{2}H, ^{12}C and ^{64}Cu, it is necessary to integrate the cross sections over the missing mass peak. In this case the cross section can be expressed (setting the interference terms to zero)

$$\int\limits_{\Delta M_x} \frac{d\sigma}{d\Omega_\pi dM_x} = \int\limits_{\Delta M_x} \frac{d\sigma_T}{d\Omega_\pi dM_x} + \epsilon \int\limits_{\Delta M_x} \frac{d\sigma_L}{d\Omega_\pi dM_x}\ , \tag{4}$$

where ΔM_x is the region of missing mass within the experimental acceptance. In the case of the free proton, the missing mass is just a radiation broadened δ function at the neutron mass. For the other target nuclei, the Fermi motion of the bound nucleons broadens the distributions, and the missing mass coverage is limited by the acceptance of the spectrometers. The upper limit of M_x in the integration will be determined to minimize the influence of pions produced above pion threshold.

The experimental cross sections will be extracted using a Monte Carlo of the experiment that includes detailed descriptions of the spectrometers, decay of the pions in flight, multiple scattering, ionization energy loss, and radiative effects. The Monte Carlo will use a model of charged pion electroproduction from nucleons to account for variations of the cross section across the acceptance. For electroproduction from ^{2}H, ^{12}C, and ^{64}Cu, this model will be implemented in a quasifree approximation in combination with realistic nucleon momentum distributions (in practice, we may include a rough or realistic [25] missing energy distribution to better describe the threshold behavior). To limit the uncertainty due to the pion electroproduction model we will take ^{1}H(e,e$'\pi^+$) data in a larger θ_{pq} and W grid than for the nuclear targets. In addition, an iterative procedure will be used to optimize the pion electroproduction model and match the resulting Monte Carlo distributions to the data.

The relatively high Q^2 and W^2 we choose for our kinematics is optimal for a number of reasons

- The missing mass coverage is larger
- The W-dependence of the cross section is smaller
- The coherent production is reduced, avoiding confusion whether to neglect or include such production
- N-N final-state interaction effects are smaller
- Pion momenta are large ($>$ 2 GeV/c), making final-state interaction effects predominantly absorptive

Even at lower Q^2 and W^2 the above mentioned procedure has been proven to work reasonably well for the ^{2}H(e,e$'\pi^+$) reaction, e.g., in the E91-003 experiment data were taken at $Q^2 = 0.4$ (GeV/c)^2 at $W = 1.60$ GeV and $W = 1.15$ GeV, corresponding to values for k, the virtual pion momentum, of 0.2 and 0.47 GeV/c, respectively. At such low values of Q^2 and W (or, more importantly, the corresponding low virtual pion momentum k) N-N final-state interaction effects can not be neglected, and were incorporated via a simple Jost function prescription. For details please see Ref. [26]. Please note that such effects decrease rapidly with increasing k, e.g., for the ^{2}H(e,e$'\pi^+$) case, at $k = 0.47$ GeV/c, Ref. [27] estimates a less than 1% effect on the integrated yield.

Results are shown in Fig. 3. At the $k = 0.20$ GeV/c kinematics the coverage is nearly complete, while at $k = 0.47$ GeV/c a significant fraction (10-30%) of the missing mass distribution is outside the experimental acceptance. The proposed kinematics will have a nearly-complete coverage. In addition, at $Q^2 \geq 2$ (GeV/c)^2 the virtual pion momentum k will be larger than 0.4 GeV/c.

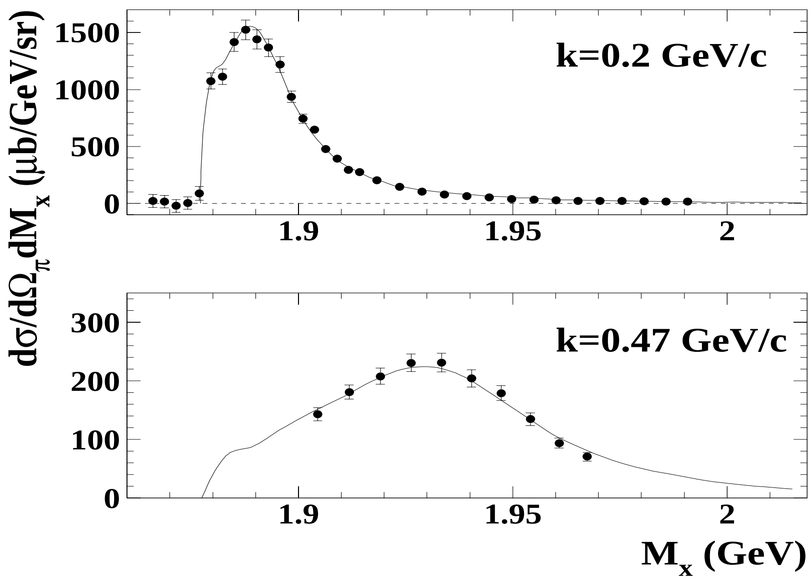

Figure 3: M_x acceptance for the ^{2}H$(e, e'\pi^+)nn$ data at low (top) and high (bottom) k. The points are cross sections with statistical errors only and curves are quasifree calculations (normalized to the data) that include N-N final state interaction effects.

The quasifree ratios will be calculated using the pion electroproduction model and momentum space wave functions used in the Monte Carlo simulation. In the case of the E91-003 experiment [26] the model dependence of the calculated ratios was estimated by comparing the results with the values obtained by using a flat cross section in place of the electroproduction model. For E91-003 the uncertainty in the quasifree calculation of the ratio varied from 2% to 10% - generally largest in the ^{3}He/H ratio [28]. Note that a large part of this uncertainty is due to the worst-case flat cross section assumption, and was inflicted on this analysis due to the lack of ^{1}H(e,e$'\pi^+$) data over a larger (θ_{pq}, W) region. Due to our choice of kinematics, we anticipate lower uncertainties, but conservatively estimate these to be between 5% and 10%. E.g., a Monte Carlo simulation with and without a W-dependence in the parameterized pion electroproduction model only changed the pion yield by 0.7%, for $W = 2.12$ GeV and $Q^2 = 1.83$ (GeV/c)^2.

An exploratory, similar, experiment to determine the kaon transparency in the nuclear medium has been performed. Ref. [29] extracted the effective number of protons participating in the quasielastic A(e,e$'$K$^+$)Λ(A-1) reaction, at $Q^2 = 0.4$ (GeV/c)^2, using the above described technique. Here, the nucleon momentum distributions used in the Monte Carlo were taken from Ji *et al.* [30]. In this case the uncertainties were dominated by statistics. The results are shown in Fig. 4. One can see that the results for the ^{12}C nucleus are in good agreement with previous Carbon photoproduction data [31]. Alternatively, one can define a kaon transparency T as the ratio of the effective number of protons $Z_{(eff)}$ to Z. The results agree well with a transparency calculation assuming a classical attenuation model, using the (inelastic) free K^+-N cross section. E.g., for the ^{12}C(e,e$'$K$^+$)Λ(A-1) case such a calculation would render a transparency of 0.66 [29].

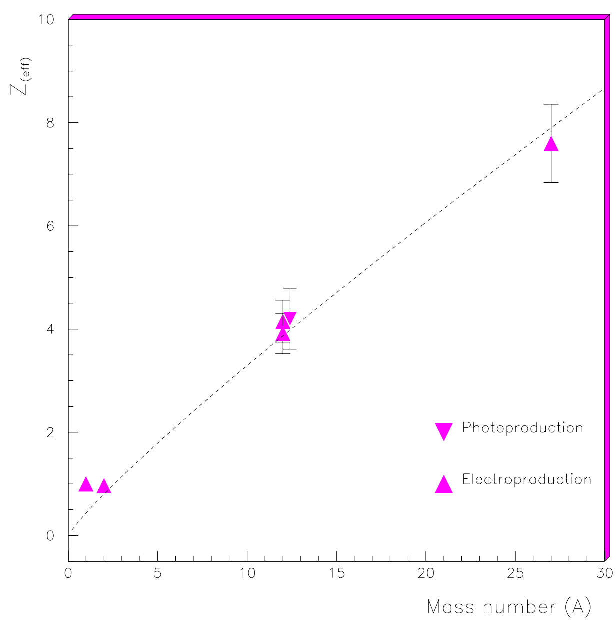

Figure 4: Effective proton number for Λ production at $Q^2 = 0.4$ (GeV/c)^2. The inverted triangle is the photoproduction data on carbon from [31]. The dashed line is a power fit Z^{α}, with $\alpha = 0.793{\pm}0.043$ [29] to the data.

2.1 Relation to Other Experiments

Three JLab experiments are closely related to the one proposed.

Experiment E99-105, "Deeply-Virtual Electroproduction of Vector-Mesons", spokespersons C. Marchand, E. Smith, and M. Guidal, is a first attempt to establish the Q^2 dependence in vector-meson electroproduction as predicted by the factorization theorems. If established, such measurements would give access to the Generalized Parton Distributions. E99-105 will obtain electroproduction data off hydrogen up to $Q^2 \approx 4$ (GeV/c)^2. A verification of the CT phenomenon for pion electroproduction at similar Q^2 would be of great benefit to this program. For pseudoscalar meson production a similar approach as proposed in E99-105 (which was, in fact, proposed as PR99-106) would require a technically more challenging Rosenbluth separation.

Experiment E91-003, and an Update Proposal to PAC 20, attempts to observe a pion excess in nuclei through "A Study of Longitudinal Charged Pion Electroproduction on H, ^{2}H, ^{3}He and ^{4}He" (spokesperson H.E. Jackson). A large pion excess would obscure the effects we are after. However, experiment E91-003, and calculations, do not find appreciable effects, even after selection, through Rosenbluth separations, of the longitudinal response function only [28]. Although pion excess effects may be measurable in the Update Proposal of E91-003, optimized to look for such effects, they are, in our kinematics, small [32] compared to the effects we look for. In addition, the A-dependence of these effects is vastly different.

Experiment E94-104, "The Fundamental $\gamma n \rightarrow \pi^- p$ Process in ^{2}H, ^{4}He, and ^{12}C in the 1.2 - 6.0 GeV Region", spokespersons H. Gao and R. Holt, used a bremsstrahlung radiator to produce a real photon beam, and tagged the γn process by detecting a pion and proton in coincidence. The experiment ran (partially) in January-March 2001, using ^{2}H and ^{4}He targets and beam energies up to 5.6 GeV (4.2 GeV for ^{4}He). The comparison of the ^{4}He target enables one to extract a pion transparency, similar as we intend to do. By detecting the pion and proton together, fermi smearing effects are negligible ensuring the exclusivity of the reaction. In addition, the CT effect may be enhanced. The CT effects for this process have been calculated by Gao *et al.* [33]. Experiment E94-104 is complementary to this proposal. The experiment proposed here can combine the kinematic selectivity of the electron scattering process, and takes the experimental approach of varying Q^2 and the nuclear medium size A. Both dependencies should be understood. In addition, the (more recent) calculations we have taken as guidance to look for effects of CT would agree with the non-observation of CT effects from the recent JLab A(e,e′p) experiments [20], and the observation of CT effects in the di-jet experiment at $Q^2 \simeq 10$ (GeV/c)^2. Lastly, the results of E94-104 on their own could not be taken as guideline where one could strictly access Generalized Parton Distributions.

Additinally, two related experiments have been performed measuring the (proton) nuclear transparency.

Experiment E94-139, a "Measurement of the Nuclear Dependence and Momentum Transfer Dependence of Quasielastic (e,e′p) Scattering at Large Momentum Transfer", spokespersons R.G. Milner and R. Ent, investigated the proton nuclear transparency through the nuclear medium up to $Q^2 =$ 8.1 (GeV/c)^2, in a search for Color Transparency. This experiment ran in 1999, and data analysis is final. No evidence for Color Transparency is found within this range of Q^2 [20].

E94-139 was the high Q^2 companion experiment of Experiment E91-013, "The Energy Dependence of Nucleon Propagation in Nuclei as Measured in the (e,e′p) Reaction", spokesperson D.F. Geesaman. Results, up to $Q^2 = 3.3$ (GeV/c)^2, have been published [19, 34].

3 Count Rate and Running Time Estimates

For the remainder of this Section we will present the choice of kinematics for this experiment, the count rate estimates, and the beam time request. We will not dwell on issues such as singles rates and particle identification. The total singles rates are well (over a factor of ten) below the capability (conservatively ≈ 0.5 MHz) of the detector packages. Separation of e^+, π^+, and K^+ is easily do-able using coincidence timing. As an example, we show an illustrative coincidence time spectrum at similar kinematics, $W = 2.4$ GeV and $Q^2 = 2.4$ (GeV/c)^2, for the ^{2}H(e,e′π^+) reaction in Fig. 5.

Additionally, we are constructing an aerogel detector for the HMS, with two choices of aerogel material ($n = 1.015$, and $n = 1.030$). This HMS aerogel is under construction for approved experiments E00-108 ("Duality in Meson Electroproduction", spokespersons R. Ent, H. Mkrtchyan, and G.

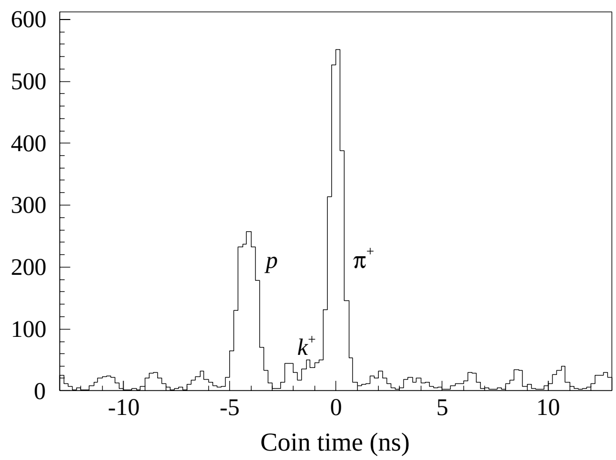

Figure 5: A coincidence time spectrum. there is a small kaon peak (just visible) at -1 ns. The 2 ns RF structure of the electron beam is visible in the multiple accidental peaks.

Niculescu) and experiment E01-004 ("Extension to E93-021: the Charged Pion Form Factor", spokespersons G. Huber, D. Mack, and H.P. Blok), and will be available early 2002. This aerogel detector, in combination with timing within the spectrometer and the existing shower counter and gas cherenkov, will allow for complete e^+, π^+, K^+, and p identification within the HMS spectrometer, for our momenta of interest.

3.1 Kinematics

We already listed the advantages of choosing kinematics at high W and high Q^2 in Section 2. Our kinematics have been constrained by the following:

- $W \geq 2$ GeV.
- Q^2 in the region of interest (see Fig.1), from $Q^2 = 1$ (GeV/c)^2 to as high as realistically possible (≈ 5 GeV/c)^2).
- Almost-parallel kinematics, such that the σ_{LT} and σ_{TT} interference terms are small, and to enable (close-to) complete ϕ_{pq} coverage.

- The conjugate angle θ_q larger than 9° (the HMS can only rotate to 10.5° minimum).

- t_{min} as low as possible, to enable minimization of possible rescattering contributions.

- Energies optimized to reflect pass-changes only, no change of base linac energy.

In addition, we have chosen the energies to enable us to perform a longitudinal-transverse (L-T) separation at $Q^2 \approx 2$ (GeV/c)^2. This is an important check of our experimental procedure, described in Section 2, to verify that the L-T character does not appreciably change from the hydrogen case to an $(A > 1)$ nuclear target case. Data from the E91-003 experiment [28] have shown that, at $Q^2 = 0.4$ (GeV/c)^2, there is no statistical evidence for such a change comparing the ^{1}H(e,e$'\pi^+$), ^{2}H(e,e$'\pi^+$) and ^{3}He(e,e$'\pi^+$) reactions (there does exist evidence for a nuclear dependence in the case of π^- electroproduction at $k = 0.20$ GeV/c [28]). Nonetheless, we wish to guarantee this also at the higher Q^2. The choice $Q^2 \approx 2$ (GeV/c)^2 is given by the combination of the practical limitation of a less-than 6 GeV beam energy and the reduced beam time needed to accumulate sufficient statistics.

We wish to mention here that, from kinematics to kinematics, both Q^2 change and t_{min} changes. Both will undoubtedly affect the actual L-T ratio of the data, but this does not affect the extracted pion transparencies as long as the L-T ratio of the free hydrogen pion electroproduction case is the same as that for the $(A > 1)$ nuclear target case. In addition, the variation of t_{min} may make one more susceptible to rescattering contributions, e.g. through ρ electroproduction followed by $\rho N \rightarrow \pi N'$ rescattering. For this reason we propose to measure two kinematics at $Q^2 = 4$ (GeV/c)^2, at varying t_{min}, to check for consistency.

Figure 6 depicts the symmetrical ϕ coverage necessary to extract the σ_{LT} and the σ_{TT} terms in order to make the Rosenbluth separation of the σ_L and σ_T terms of the cross section for the Q^2=1.83 GeV^2/c^2, $\epsilon = 0.60$ and $W = 2.12$ GeV^2/c^2. From Table 1 it is evident that good ϕ coverage will be obtained for most kinematic settings. Exceptions are the kinematics where $\theta_{HMS} > \theta_\pi$, i.e. at Q^2=1.83 GeV^2/c^2 and $\epsilon = 0.26$, at Q^2=4.0 GeV^2/c^2 and

ϵ = 0.30, and at Q^2=5.0 GeV^2/c^2. This is due to the mechanical limitation of the minimum HMS angle to θ_{HMS}=10.5°.

An alternative check would be to measure the π^+/π^- ratio off nuclear targets. However, within our approach we do not require pole-term dominance. Also, the existing data, be it limited, do not reflect an appreciable nuclear dependence of such ratio [35, 36].

The beam energies chosen are 3.54 GeV, 4.70 GeV, and 5.86 GeV, for a base linac energy of 1.16 GeV/pass. The latter is not critical, but will only slightly change the choices of Q^2 and W. The kinematics are further specified in Table 1.

Table 1: Kinematics for the measurement of pion transparency in nuclei. The kinematics labeled with an asterisk (*) is added to verify a possibly (W,k) dependence, with k the virtual pion momentum.

Q^2 GeV^2	W GeV	t GeV^2	E_e GeV	$\theta_{e'}^{SOS}$ deg	$E_{e'}$ GeV	θ_π deg	θ_{HMS} deg	p_π GeV	k GeV	ϵ
1.00	2.10	-0.053	3.54	29.00	1.126	12.06	12.06	2.380	0.23	0.52
1.83*	1.70	-0.304	3.54	34.21	1.494	20.02	20.02	1.877	0.56	0.62
1.83	2.12	-0.137	3.54	53.46	0.639	9.23	10.50	2.823	0.39	0.26
1.83	2.12	-0.137	4.70	27.33	1.770	14.61	14.61	2.823	0.39	0.60
3.00	2.10	-0.301	4.70	42.40	1.220	12.22	12.22	3.315	0.58	0.40
4.00	2.15	-0.422	5.86	36.56	1.734	13.02	13.02	3.897	0.71	0.47
4.00	2.40	-0.295	5.86	45.78	1.128	9.05	10.50	4.571	0.58	0.30
5.00	2.22	-0.523	5.86	53.90	1.038	9.08	10.50	4.540	0.79	0.26

3.2 Count Rate Estimates

In the count rate estimates, we assumed the use of 4 cm long cryogenic hydrogen and deuterium targets, Al dummy targets for window subtraction, a solid ^{12}C foil of 2% radiation length, a solid ^{64}Cu foil of 6% radiation length,

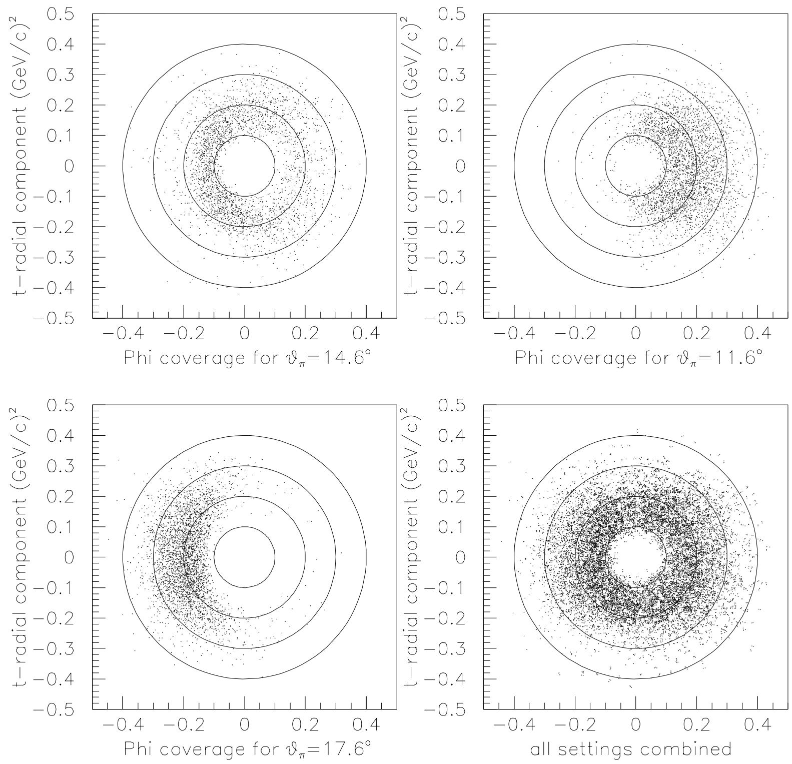

Figure 6: The azimuthal angle, ϕ, coverage versus $-t$ at Q^2=1.83 GeV^2/c^2 and $\epsilon = 0.60$. The polar plots depict $-t$ as the radius versus ϕ where each radial division corresponds to $-t = 0.1$ GeV^2/c^2. The upper left panel represents the ϕ coverage for the parallel kinematic setting of $\theta_{\pi q}$=14.6°. Here the coverage is predominantly centered about $\phi = 180^o$. The upper right panel $\theta_{\pi q}$=11.6^o yields data approximately center about $\phi = 0°$. Lower left panel shows the additional ϕ coverage obtained for $\theta_{\pi q}$=17.6°. Lower right panel is the superposition of all there kinematical settings depicting good ϕ coverage for $0.1 < |t| < 0.3$ GeV^2/c^2.

and a solid ^{197}Au foil of 12% radiation length. In addition, we assume a beam current of 50 μA.

We used the Hall C Monte Carlo package SIMC to estimate the ^{1}H(e,e$'\pi^+$)n count rates. This Monte Carlo includes detailed descriptions of the spectrometers, decay of the pions in flight, multiple scattering, ionization energy loss, and radiative effects, and is in fact (almost) the same Monte Carlo that will be used for the final data analysis and iterative procedures.

Count rate estimates for the ^{1}H(e,e$'\pi^+$) kinematics are given in Table 2. In addition, we present the number of hours requested for the ^{1}H(e,e$'\pi^+$)n part of the experiment. We aim for a statistical uncertainty of 1% for $Q^2 \leq$ 3 (GeV/c)^2 in integrated yields, 1.4% at Q^2 = 4 (GeV/c)^2 and 1.7% for Q^2 = 5 (GeV/c)^2. Obviously, this statistical uncertainty is smaller than the estimated 5 to 10% model-dependency of the results, as statistical precision is required to minimize the latter.

Table 2: Coincident rates in parallel kinematics for the ^{1}H(e,e$'\pi^+$)n reaction. The rates are based on the real detector acceptance incorporated in the simulation package SIMC for HMS and SOS spectrometers. The rates assume a 50 μA beam current and a 4.0 cm LH_2 target. The kinematics labeled with an asterisk (*) is added to verify a possibly (W,k) dependence.

Q^2 GeV^2	W (GeV)	ϵ	Hours per 10 K events	Statistics %	Run time (hours)
1.00	2.10	.52	0.4	1.0	1
1.83*	1.70	.62	1.5	1.2	1
1.83	2.12	.26	7.7	1.0	8
1.83	2.12	.60	0.7	1.0	1
3.0	2.10	.40	5.0	1.0	5
4.0	2.15	.47	5.1	1.4	3
4.0	2.40	.30	12.5	1.4	6
5.0	2.22	.26	36.4	1.7	13

To estimate the beam time required for target nuclei other than ^{1}H, we define a figure-of-merit (FOM), defined as $t/A \times Z \times T$, with t the target thickness in g/cm^2, A the nucleon number, Z the proton number (as exclusive π^+ electroproduction only occurs off the protons), and T an estimated pion transparency number based upon the values given at $Q^2 = 1$ (GeV/c)^2 of Fig. 1. The beam time we require is based upon the ratio of this FOM with respect to the FOM of hydrogen running. The exception to this rule are the data required for Al(e,e$'\pi^+$) running, as we do not intend to use ^{27}Al as a physics target, but rather only use these "Dummy" targets for the subtraction of events originating from the cryogenic target walls for hydrogen and deuterium running. We present the assumed target thicknesses, derived FOM's, and ratios of beam time requested with respect to hydrogen running, in Table 3.

Table 3: Assumed target thicknesses and derived FOM's (see text) for the quasifree A(e,e$'\pi^+$)n(A-1) reaction. The last column represents the ratio of beam time required for the nuclear targets, normalized to the ^{1}H(e,e$'\pi^+$)n case, to obatin comparable statistics as given in Table 2. Note that we require less statistics for the Al or "Dummy", case, as we only use this data for subtraction of the cryotarget wall yields.

Target	Thickness rl (%)	FOM	Run time to LH_2 time
H	0.5	0.28	1.0
D	0.5	0.29	1.0
C	2	0.24	1.2
Cu	6	0.14	2.0
Au	12	0.09	3.2
Al	2.3	0.13	0.5

Lastly, as mentioned before, we require kinematics at additional W and θ_{pq} for the ^{1}H(e,e$'\pi^+$)n case, to have large enough kinematic region to constrain the pion electroproduction model for the Fermi-smeared A(e,e$'\pi^+$) data. We assume we can live with less statistical precision ($\times 2$) in these additional runs. Therefore, we have added another cycle of ^{1}H(e,e$'\pi^+$)n running as overhead to the requested beam time.

3.3 Beam Time Request

The total beam time requested is 408 hours or 17 days (see Table 4). Of these 408 hours, 358 are for production running. We request three different beam energies, of 3-pass, 4-pass, and 5-pass, with a base linac energy of 1.16 GeV/pass. We assume a change of pass to require an additional 4 hours each, or 8 hours total. Additonally, we added 23 hours for various kinematic changes (an hour each for each kinematics in Table 1, plus half an hour each for the additional ^{1}H(e,e$'\pi^+$) kinematics). We intend to add the (few) solid targets we require to the cryogenic target ladder, minimizing the time required to change targets. Thus, no additional time has been requested for such target changes. Lastly, we do not include beam time for optics calibration of the SOS spectrometer at a saturation momentum of 1.76 GeV/c, as this is already included in approved experiment E01-004.

Table 4: Summary of beam time request.

Target	Purpose	Time hr
H	Production	38
H	(W,θ_{pq}) Range	38
D	Production	38
Al	Wall subtraction	19
C	Production	46
Cu	Production	76
Au	Production	122
–	Pass Changes	8
–	Kinematics Changes	23

References

[1] S.J. Brodsky, L. Frankfurt, J.F. Gunion, A.H. Mueller, and M. Strikman, Phys. Rev. D **50**, 3134 (1994).

[2] J. Collins, L. Frankfurt, and M. Strikman, Phys. Rev. D **56**, 2982 (1997).

[3] L.L. Frankfurt, P.V. Pobylitsa, M.V. Polyakov, and M. Strikman, Phys. Rev. D **60**, 014010 (1999).

[4] M. Diehl, T. Gousset, B. Pire, and O. Teryaev, Phys. Rev. Lett. **81**, 1782 (1998).

[5] X. Ji, Phys. Rev. Lett. **78**, 610 (1997); Phys. Rev. D **55**, 7114 (1997).

[6] A.V. Radyushkin, Phys. Lett. **B380**, 417 (1996); Phys. Rev. D **56**, 5524 (1997).

[7] M. Eides, L. Frankfurt, and M. Strikman, Phys. Rev. D **59**, 114025 (1999).

[8] M. Strikman, Nucl. Phys. **A663&A664**, 64c (2000).

[9] A.H. Mueller, in Proceedings of the Seventeenth Recontre de Moriond Conference on Elementary Particle Physics, Les Arcs, France, 1982, edited by J. Tran Thanh Van (Editions Frontieres, Gif-sur-Yvette, France,1982); S.J.Brodsky, in Proceedings of the Thirteenth International Symposium on Multiparticle Dynamics, Volendam, The Netherlands, 1982, edited by W. Kittel et al. (World Scientific, Singapore, 1983).

[10] L.L. Frankfurt, G.A. Miller, and M.I. Strikman, Comments Nucl. Part. Phys. **21**, 1 (1992).

[11] E.M. Aitala *et al.*, hep-ex/0010044 (2000).

[12] L.L. Frankfurt, G.A. Miller, and M.I. Strikman, Phys. Lett. **B304**, 1 (1993).

[13] M. Vanderhaeghen, P.A.M. Guichon, and M. Guidal, Phys. Rev. D **60**, 094017 (1999).

[14] A. Airapetian *et al.*, Eur. Phys. Jour. C **17**, 389 (2000).

[15] J.P. Ralston and B. Pire, Phys. Rev. Lett. **61**, 1823 (1988); Phys. Rev. Lett. **65**, 2343 (1990).

[16] A.S. Carroll *et al.*, Phys. Rev. Lett. **61**, 1698 (1988).

[17] Y. Mardor *et al.*, Phys. Rev. Lett. **81**, 5085 (1998); A. Leksanov *et al.*, hep-ex/0101039 (2001).

[18] N.C.R. Makins *et al.*, Phys. Rev. Lett. **72**, 1986 (1994); T.G. O'Neill *et al.*, Phys. Lett. **351**, 87 (1995).

[19] D. Abbott *et al.*, Phys. Rev. Lett. **80**, 5072 (1998).

[20] K. Garrow *et al.*, to be submitted to Phys. Rev. C (2001).

[21] B. Kundu, J. Samuelsson, P. Jain, and J.P. Ralston, Phys. Rev. D **62**, 113009 (2000).

[22] V.L. Chernyak and A.R. Zitnisky, Nucl. Phys. **B246**, 52 (1984).

[23] I.D. King and C.T. Sachrajda, Nucl. Phys. **B279**, 785 (1987).

[24] G. Miller, in *Proc. Workshop on Options for Color Coherence/Transparency Studies at CEBAF*, CEBAF, Newport News, May 22-23 (1995).

[25] Work is in progress to use calculations from O. Benhar to include realistic missing energy distributions (J. Arrington, private communications).

[26] D. Gaskell, Ph.D. Thesis, Oregon State University (2001).

[27] T.-S.H. Lee (private communication).

[28] D. Gaskell *et al.*, Submitted to Phys. Rev. Lett. (2001).

[29] W.L. Hinton, Ph.D. Thesis, Hampton University (2001).

[30] X. Ji and J. Engel, Phys. Rev. C **40**, 496 (1989); X. Ji and R.D. McKeown, Phys. Lett. **B236**, 130 (1990).

[31] H. Yamazaki *et al.*, Phys. Rev. C **52**, R1157 (1995).

[32] G.A. Miller, nucl-th/0104025 (2001).

[33] H. Gao, R.J. Holt, and V.R. Pandharipande, Phys. Rev. C **54**, 2779 (1996).

[34] D. Dutta *et al.*, Phys. Rev. C **61**, 061602(R) (2000).

[35] J.F. Martin and L.S. Osborne, Phys. Rev. Lett. **38**, 1993 (1977).

[36] H. Mkrtchyan (private communication).